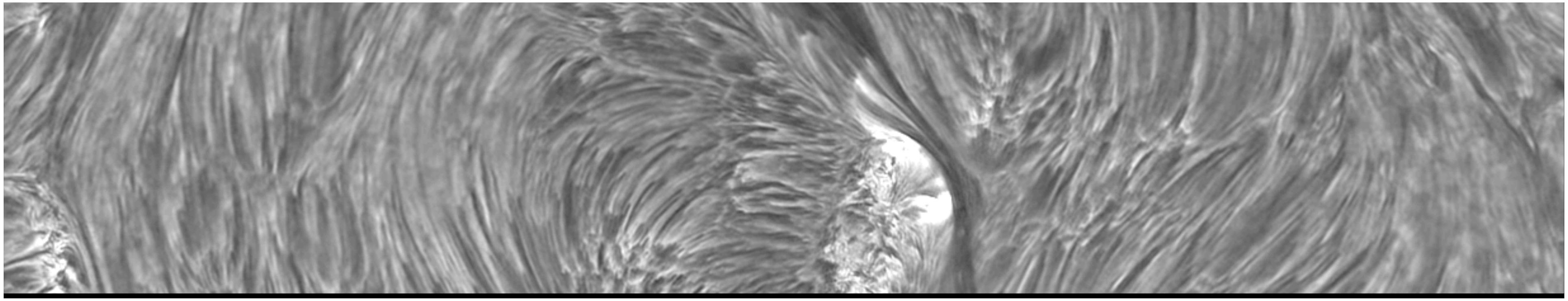

Rayleigh–Taylor instability in partially ionized prominence plasma

E. Khomenko, A. Díaz, A. de Vicente, M. Collados & M. Luna

Departamento de Astrofísica, Universidad de La Laguna and
Instituto de Astrofísica de Canarias (IAC),

La Laguna, Tenerife (Spain).

Main Astronomical Observatory, NAS, Kiev, (Ukraine)

SPIA
Solar Partially Ionized Atmosphere

http://www.iac.es/proyecto/spia/

Universidad de La Laguna

Observations of instabilities

HINODE observations of quiescent solar prominence

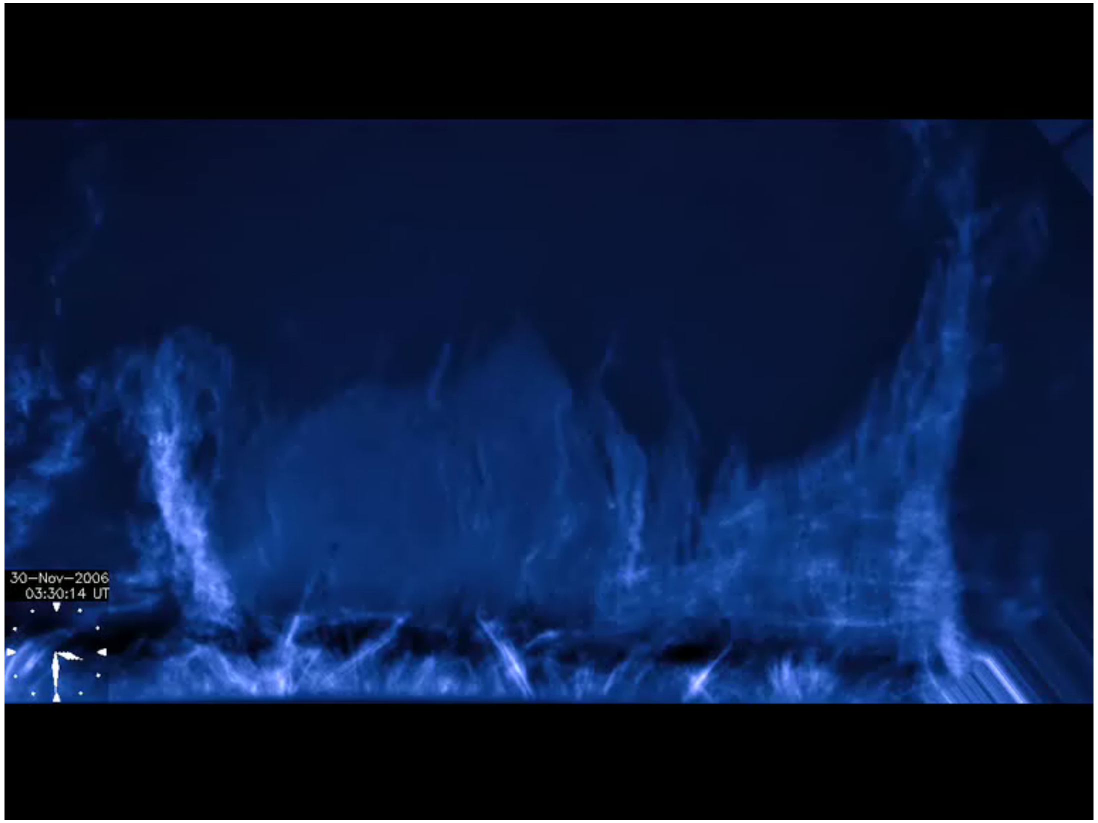

Berger et al. 2008

Linear theory of magnetic RTI

Linear growth rate (Chandrasekhar 1961)

$$\omega^2 = -gk\frac{\rho_2-\rho_1}{\rho_2+\rho_1} + \frac{2(\boldsymbol{B}_0\boldsymbol{k})^2}{\mu(\rho_2+\rho_1)}$$

Critical wavelength below which instability is completely suppressed

$$\lambda_c = \frac{B_0^2\cos^2\theta}{(\rho_2-\rho_1)g}$$

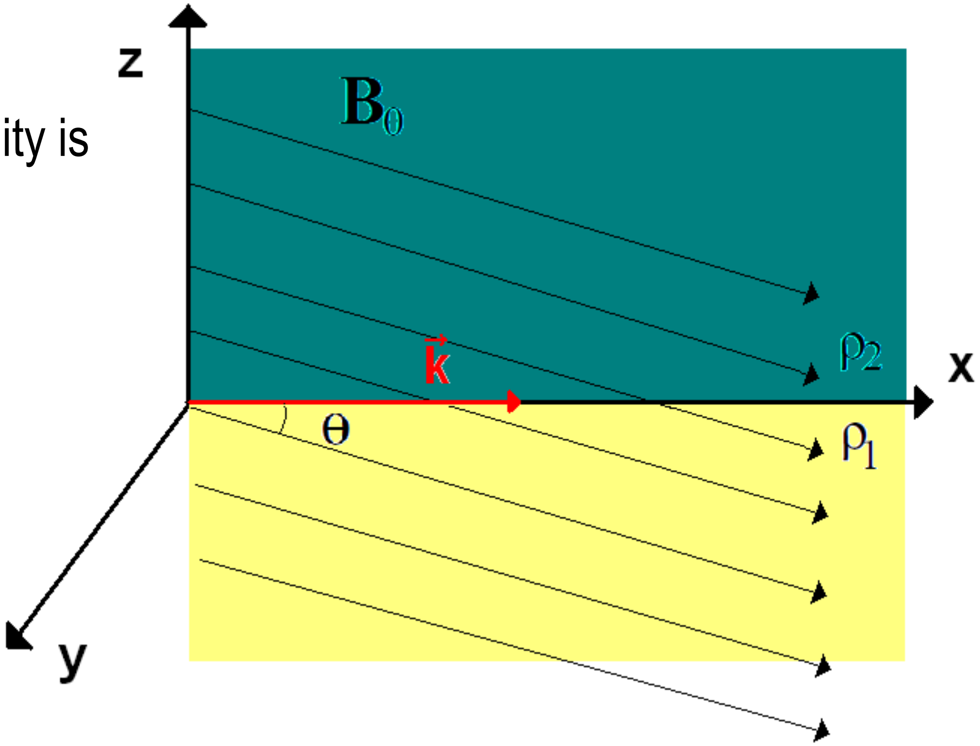

Magnetic RTI in partially ionized plasma

Prominence material is only partially ionized

Deviations from classical MHD are expected

Single-fluid vs multi-fluid approach

Only linear theory has been developed so far

Multi-fluid: Díaz et al. (2012), Soler et al. (2012)

Single-fluid: Díaz, Khomenko & Collados (2013)

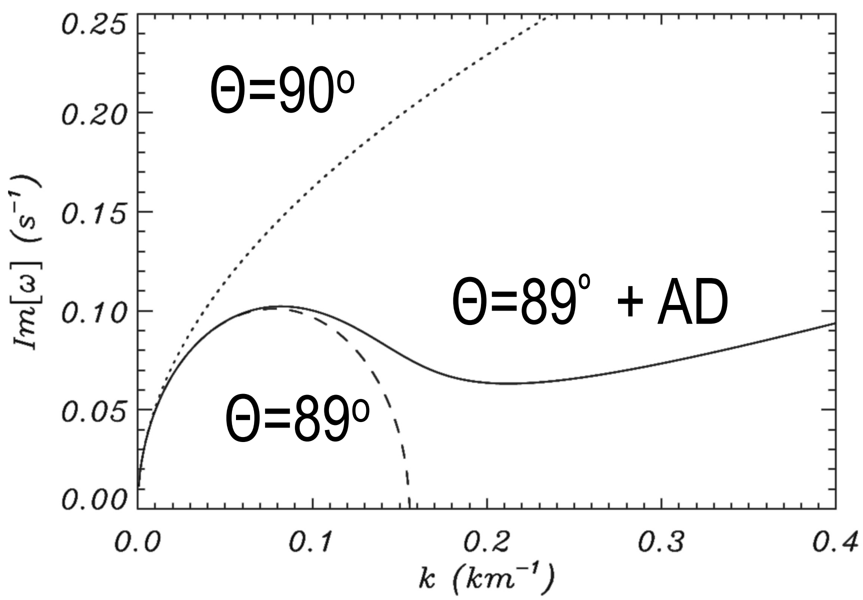

Elena Khomenko

No critical wavelength, plasma always unstable

Single-fluid quasi-MHD equations

$$\frac{\partial \rho}{\partial t} + \vec{\nabla}\left(\rho \vec{u}\right) = 0$$

Mass conservation

$$\rho \frac{D\vec{u}}{Dt} = \vec{J} \times \vec{B} + \rho \vec{g} - \vec{\nabla} p$$

Momentum conservation

$$\frac{De_{\rm int}}{Dt} + \gamma e_{\rm int} \vec{\nabla} \vec{u} = \vec{J}\vec{E}^*$$

Energy conservation

+ Generalized Ohm's law:

Assumes strong collision coupling between the species

$$\vec{E}^* = \left[\vec{E} + \vec{u} \times \vec{B}\right] = \boxed{\eta \vec{J}} + \boxed{\eta_H \left[\vec{J} \times \vec{b}\right]} - \boxed{\eta_A \left[(\vec{J} \times \vec{b}) \times \vec{b}\right]}$$

Ohmic term **Hall term** **Ambipolar term**

Simulation setup

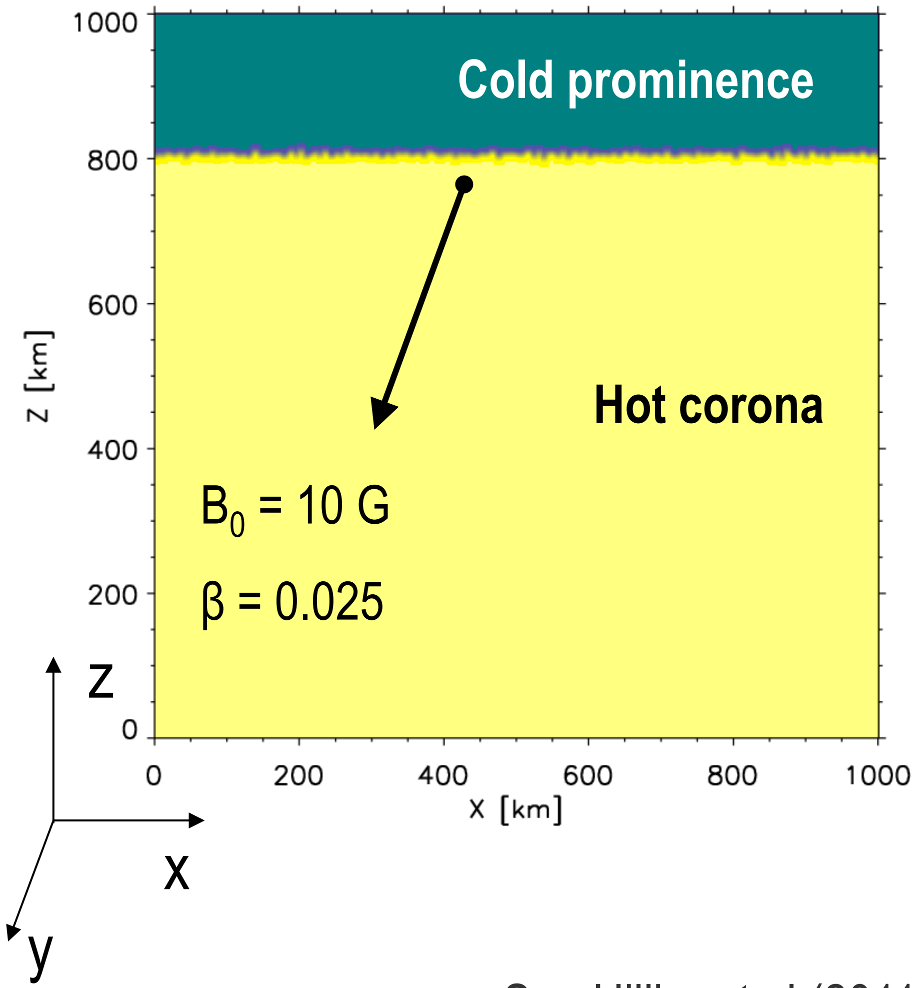

$T \approx 5000$ K; $\rho \approx 3\times10^{-13}$ g cm^{-3}

Neutral fraction $\rho_n/\rho \approx 0.9$

$T \approx 400.000$ K; $\rho \approx 4\times10^{-15}$ g cm^{-3}

Neutral fraction $\rho_n/\rho = 0$

- Multi-mode perturbation of the interface
- Spatial resolution of 1 km
- Generalized Ohm's law (ambipolar term "on")

See Hillier et al (2011, 2012) for 3D MHD simulations of RTI in Kippenhahn-Schlüter prominence model

θ= 89.9º to the perturbation plane

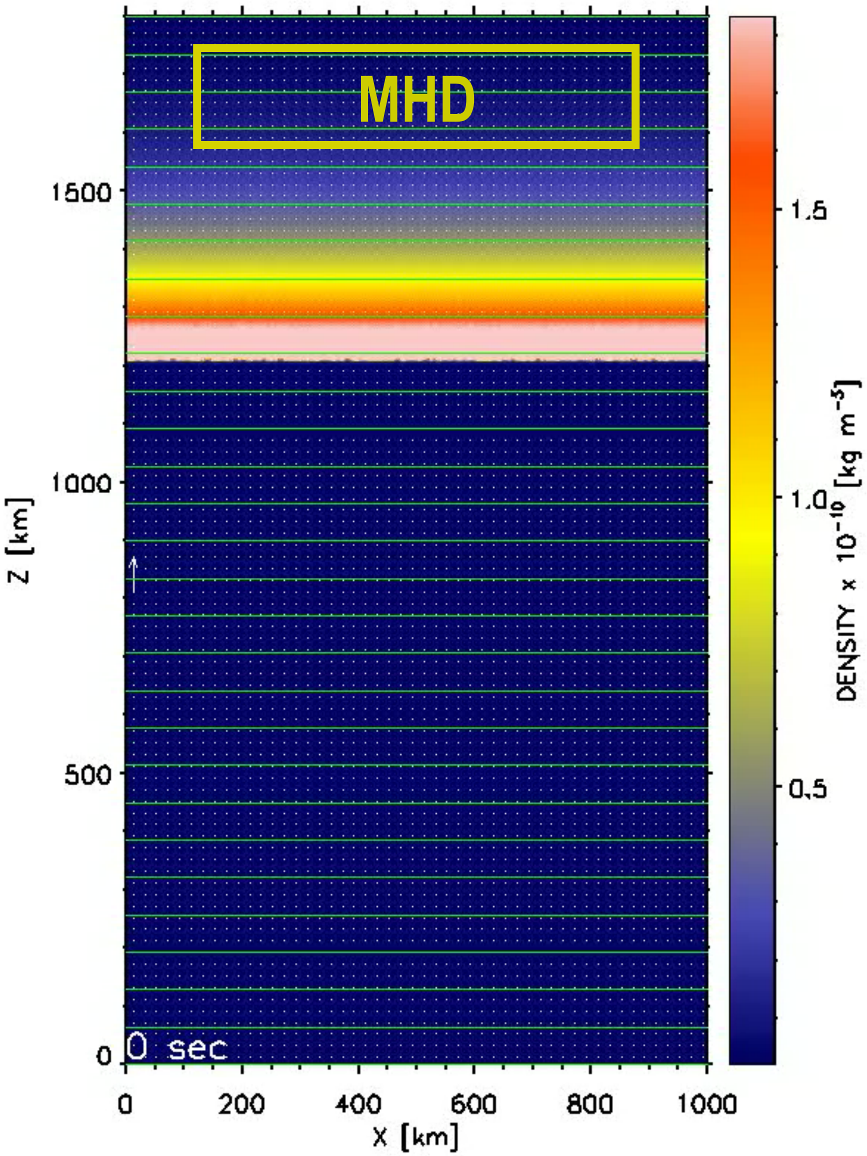

B

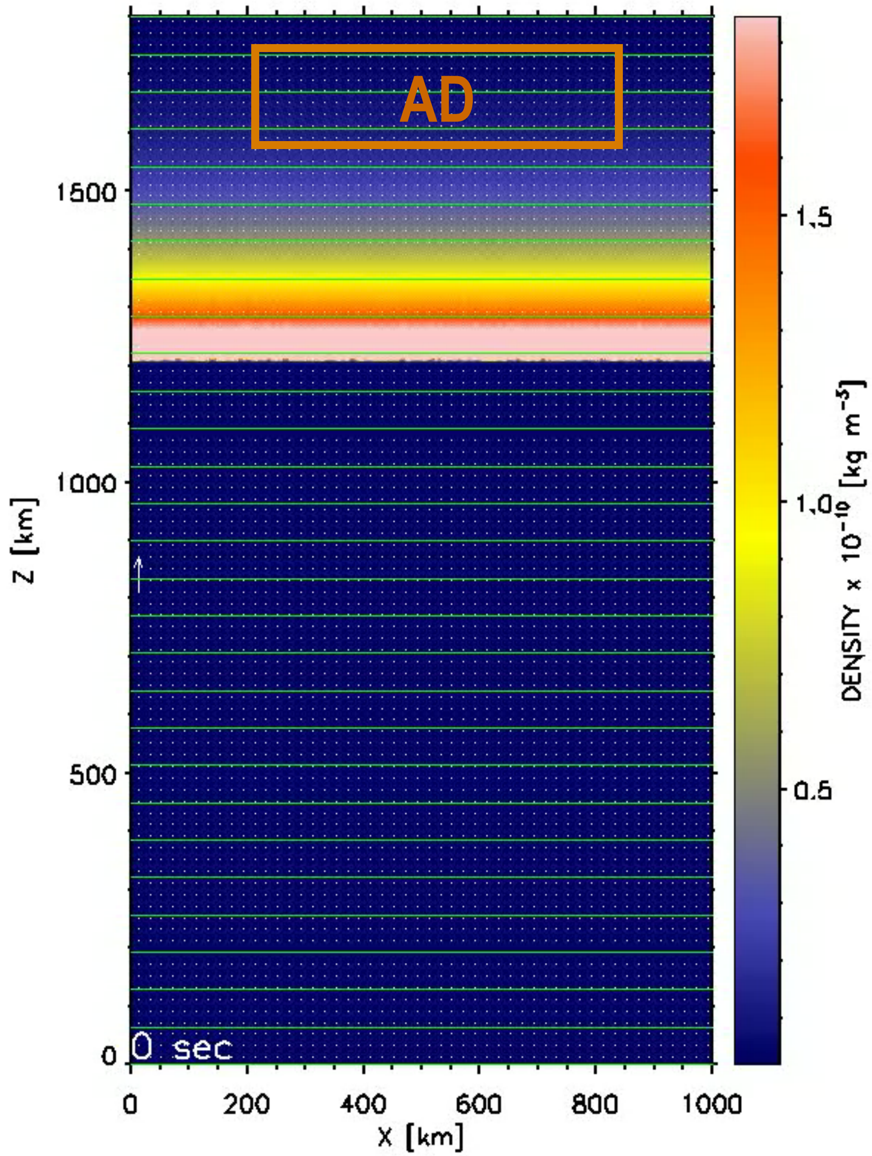

B_0 inclined away from normal to the plane

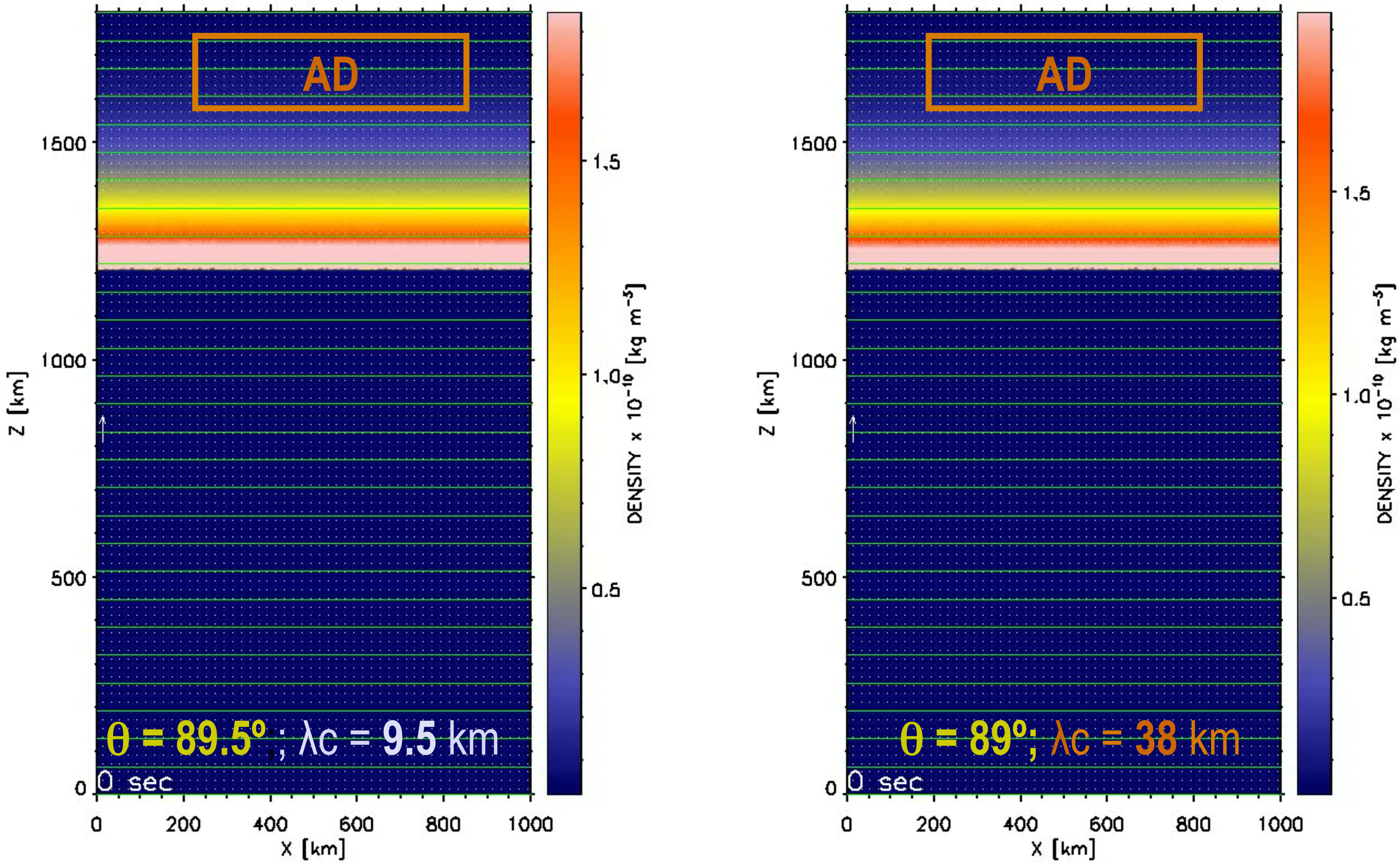

B_0 inclined away from normal to the plane

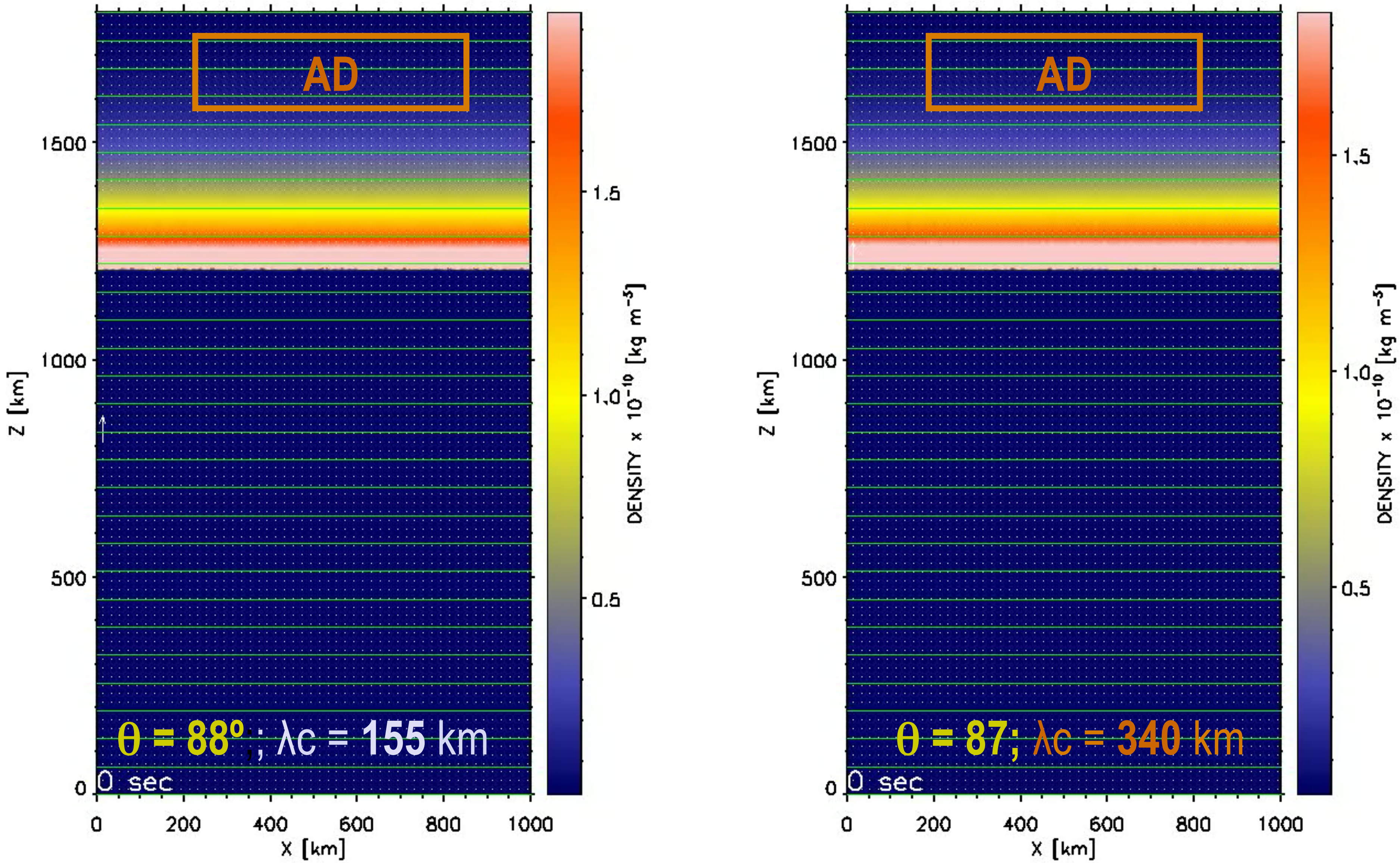

3D field lines

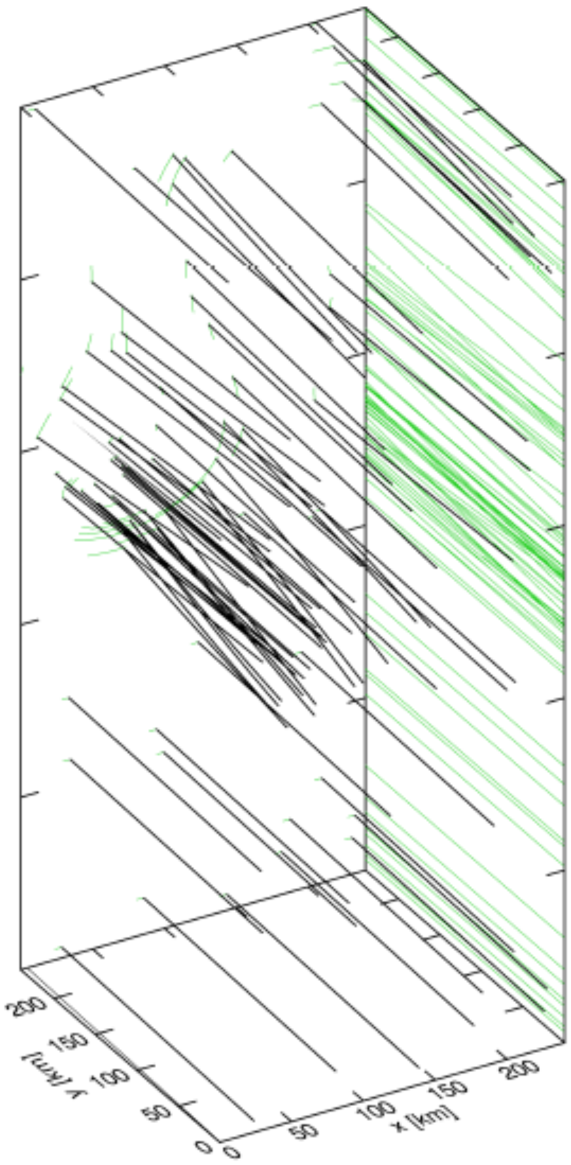

Elena Khomenko

SPIA
Solar Partially Ionized Atmosphere

Growth rate of RTI modes

Small-scales appear first:

faster linear growth rate

Large-scales dominate later:

non-linear bubble interaction

Small-scales are suppressed by magnetic tension force

Field compression additionally increases λ_C

see Jun et al. (1995)

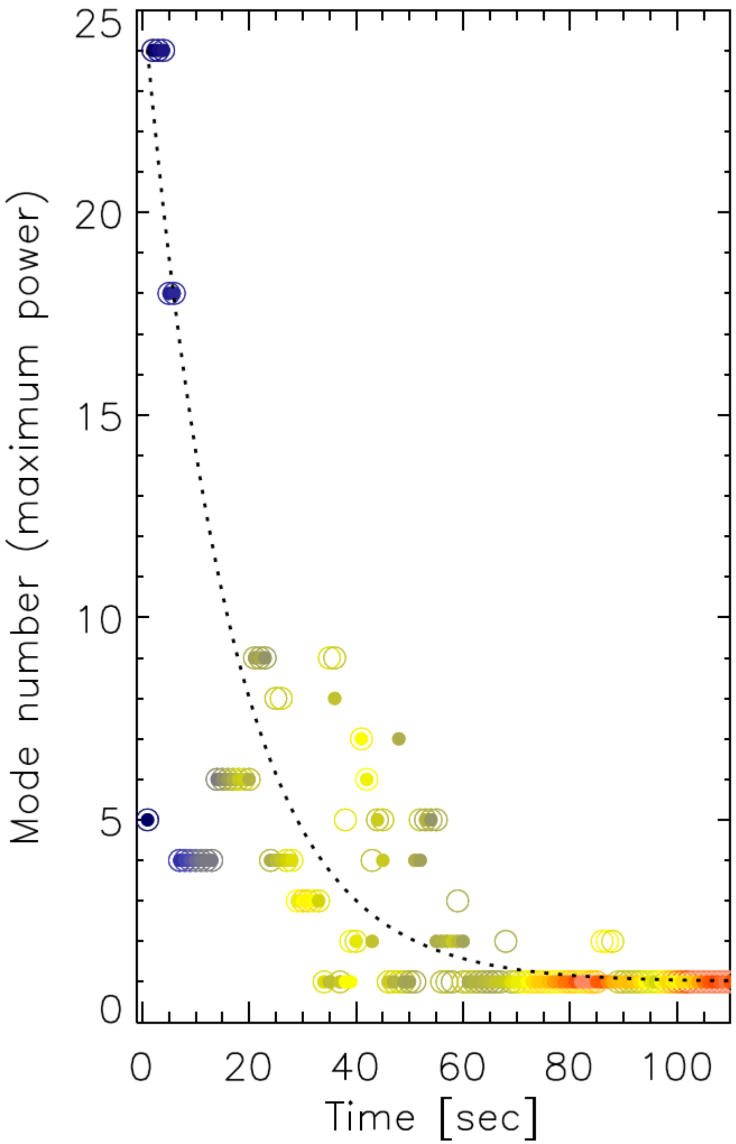

Velocity distribution in ~linear regime, θ=89º

“ambipolar” model has slightly larger velocities in the linear regime

neutrals make plasma more unstable

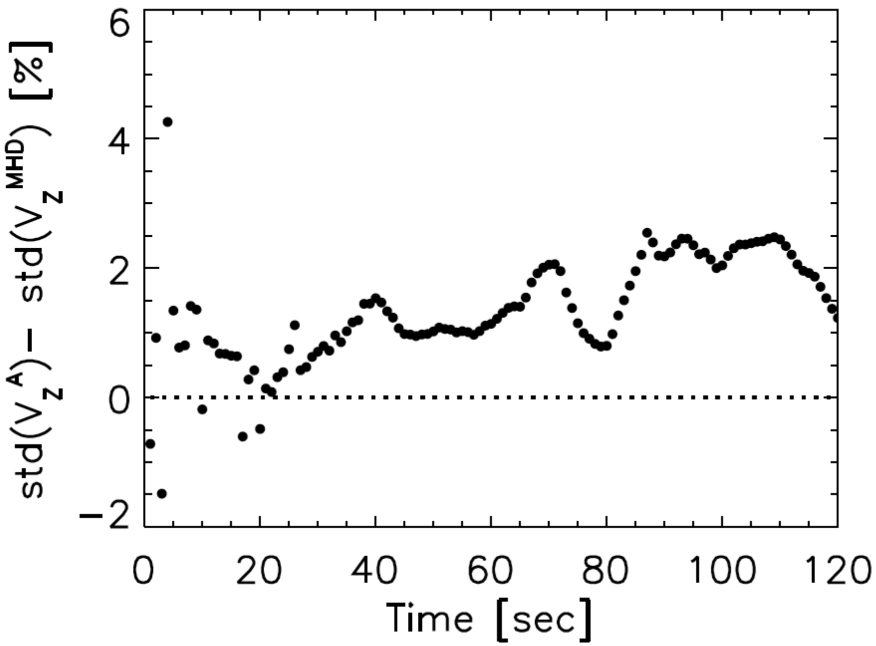

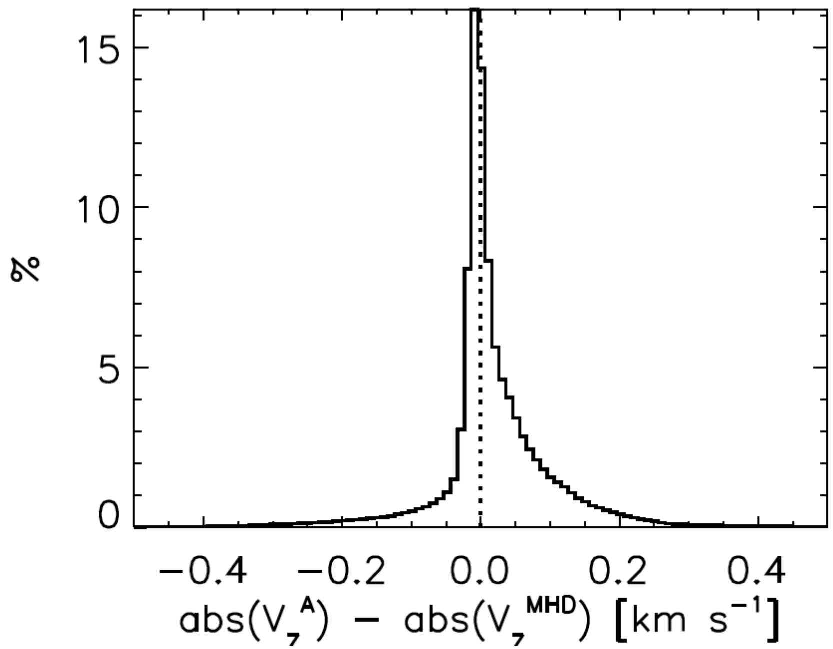

Velocity distribution in non-linear regime, $\theta=90^{o}$

Asymmetric up- and down- flow distribution, ±10-20 km s^{-1}

"ambipolar" model has more extreme velocities

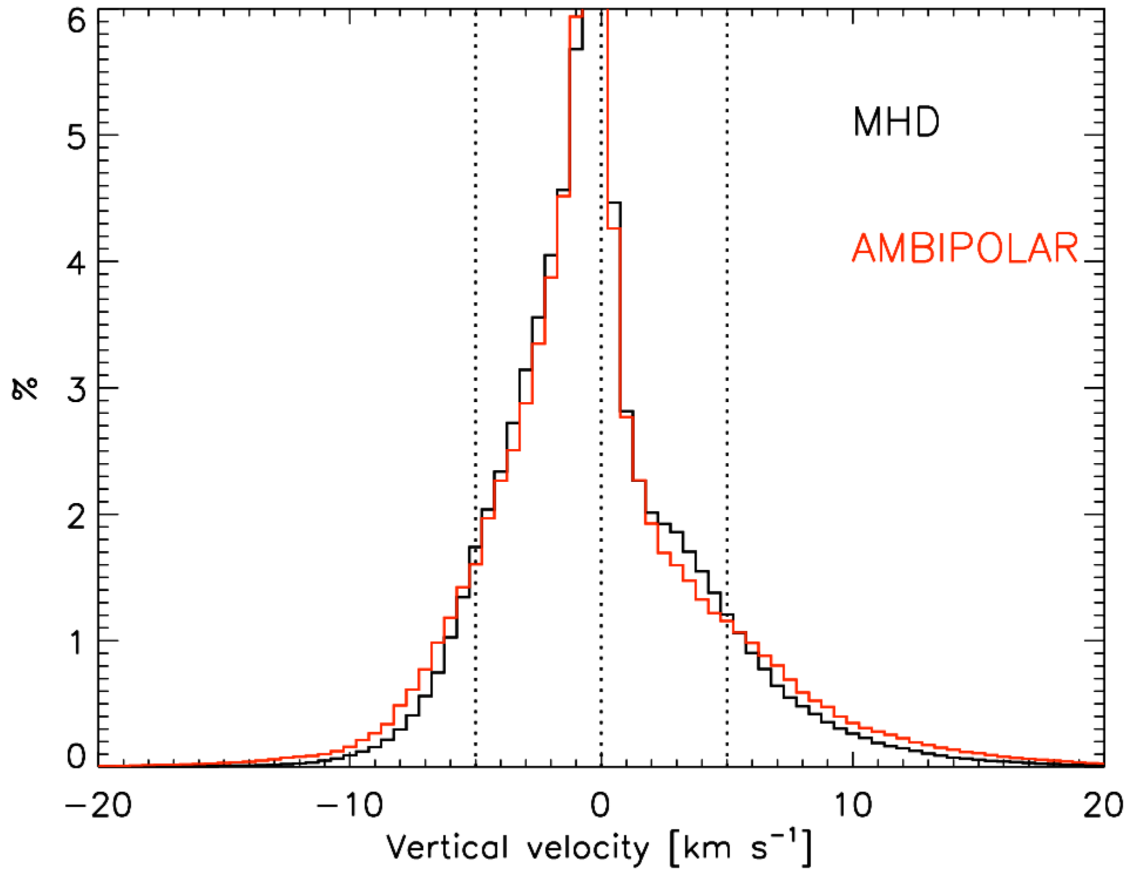

Elena Khomenko

SPIA
Solar Partially Ionized Atmosphere

Growth rate of RTI modes, θ=90°

Similar mode growth rate in “ambipolar” and “mhd” models

No critical wavelength λc

Power (ambipolar) / Power (mhd)

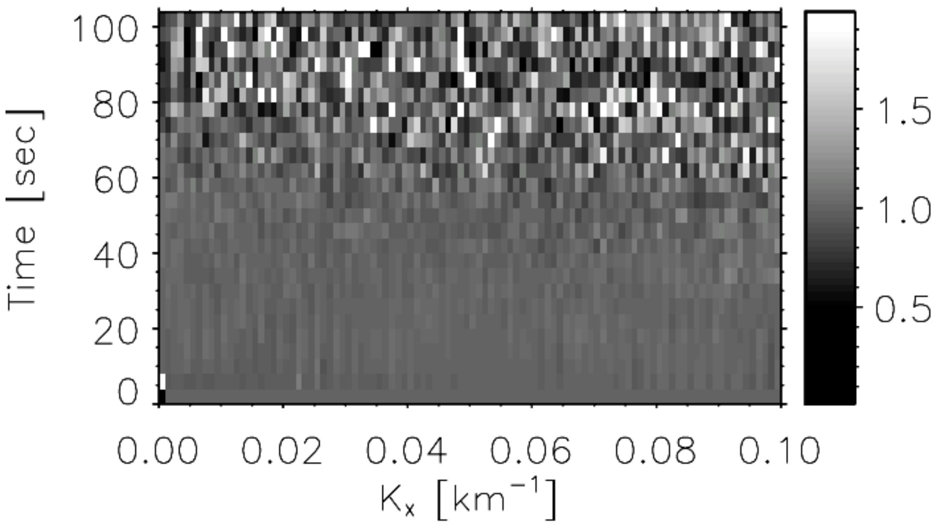

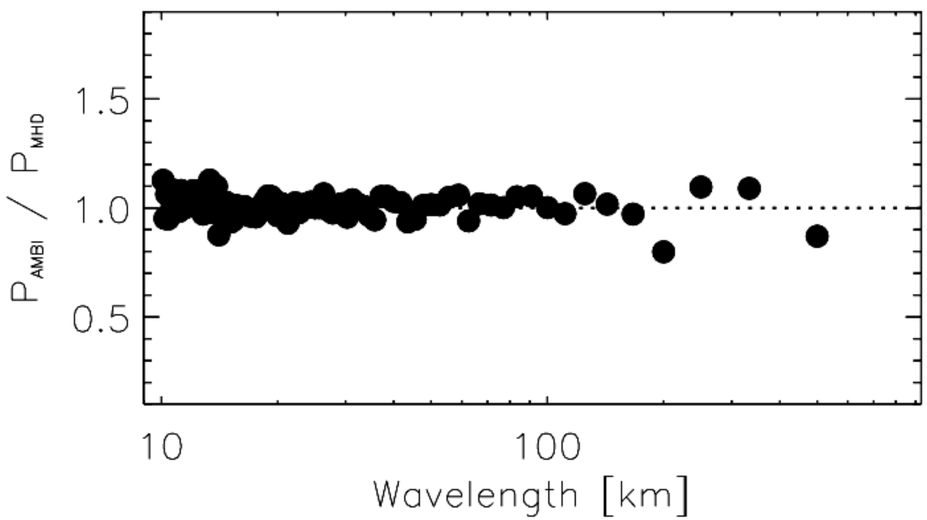

Growth rate of RTI modes, θ=89°

"ambipolar" model shows larger growth rate at small scales, compared to "mhd" model

Change of behavior at λ~λc=30 km

$$\lambda_c = \frac{B_0^2 \cos^2\theta}{(\rho_2 - \rho_1)g}$$

Power (ambipolar) / Power (mhd)

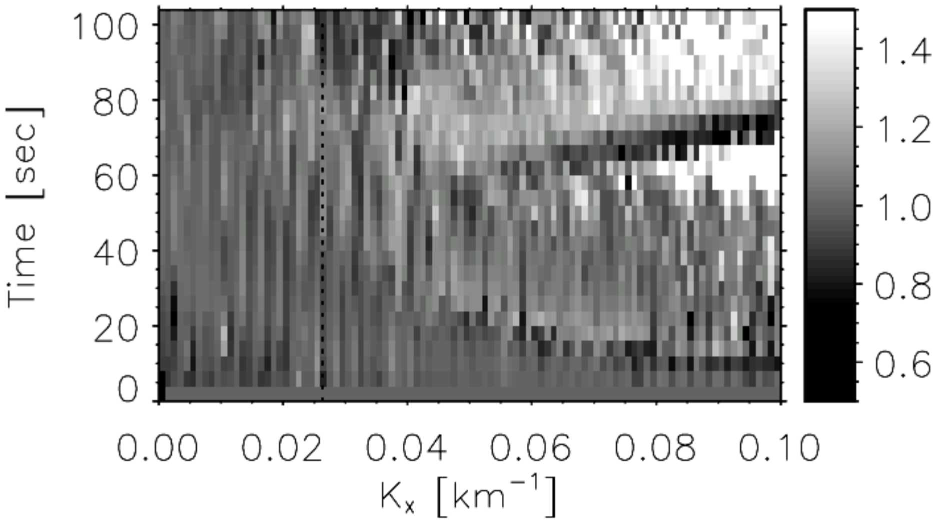

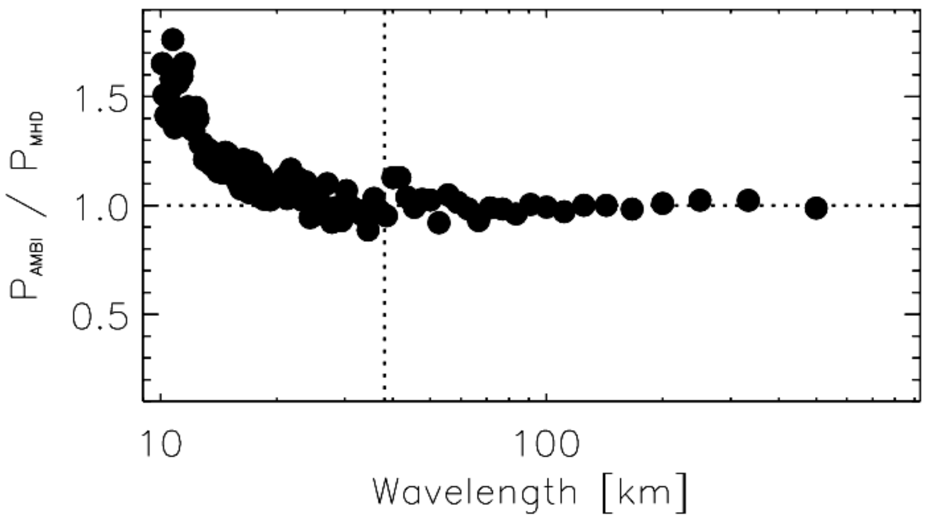

Growth rate of RTI modes, θ=88°

"ambipolar" model shows larger growth rate at small scales, compared to "mhd" model

Change of behavior at $\lambda \sim \lambda_c = 100$ km

$$\lambda_c = \frac{B_0^2 \cos^2\theta}{(\rho_2 - \rho_1) g}$$

Power (ambipolar) / Power (mhd)

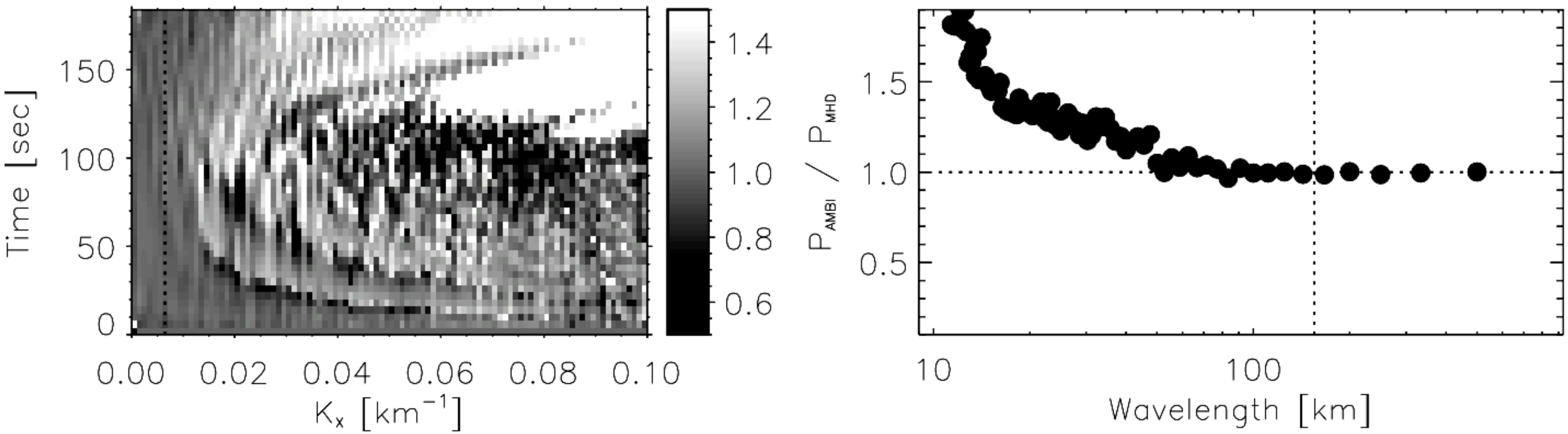

Elena Khomenko

SPIA Solar Partially Ionized Atmosphere

Temperature difference “mhd” vs “ambipolar”

Chromospheric material is more than 30% hotter in the “ambipolar” model (Joule heating due to current dissipation)

B=10 G, θ=89º

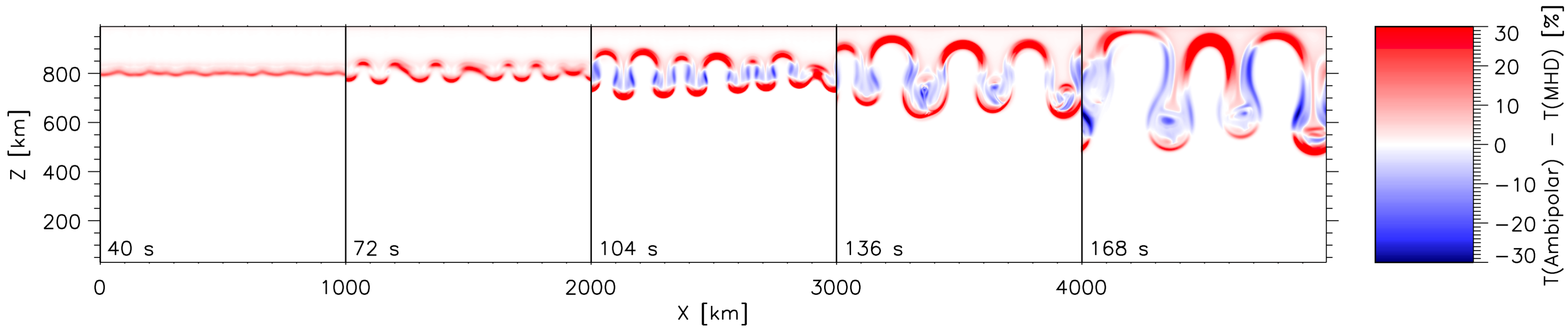

Elena Khomenko

Diffusion velocity $\boldsymbol{w} = \boldsymbol{u}_i - \boldsymbol{u}_n$

$$\boldsymbol{w} = \boxed{\frac{\xi_n}{\alpha_n}[\boldsymbol{J} \times \boldsymbol{B}]} - \boxed{\frac{(2\xi_n \boldsymbol{\nabla} p_e - \xi_i \boldsymbol{\nabla} p_n)}{\alpha_n}}$$

Currents Gradients of partial pressures

Negative values: neutrals fall faster than ions by a few km s^{-1}

Inclination θ=89º

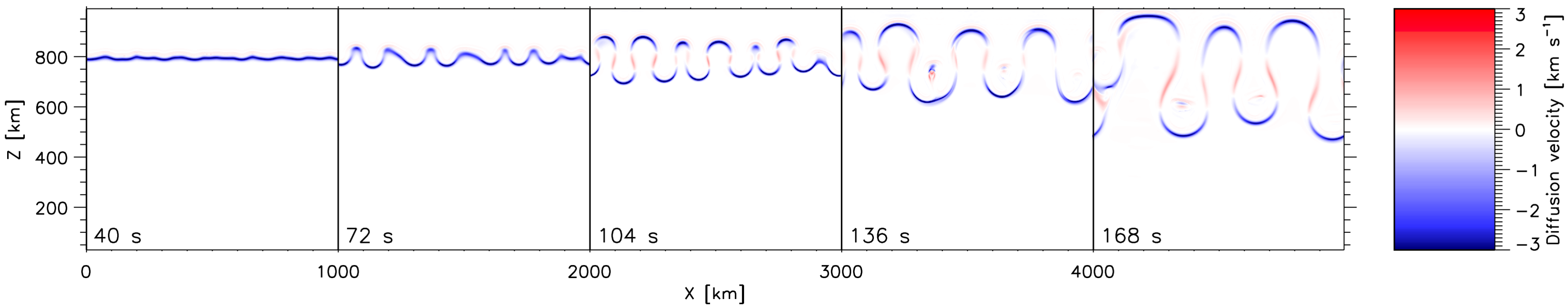

Diffusion velocity $\boldsymbol{w} = \boldsymbol{u}_i - \boldsymbol{u}_n$

$$\boldsymbol{w} = \boxed{\frac{\xi_n}{\alpha_n}[\boldsymbol{J}\times\boldsymbol{B}]} - \boxed{\frac{(2\xi_n\boldsymbol{\nabla}p_e - \xi_i\boldsymbol{\nabla}p_n)}{\alpha_n}}$$

Currents

Gradients of partial pressures

Negative values: neutrals fall faster than ions by a few km s^{-1}

Inclination θ=90º

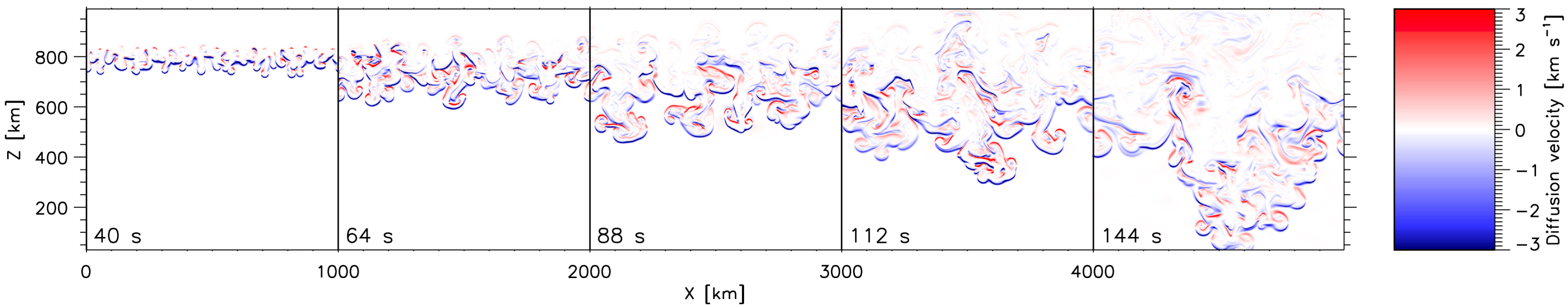

Ion-neutral momentum

$$\boldsymbol{p}_D = \sqrt{(\rho_i \rho_n)}\boldsymbol{w}.$$

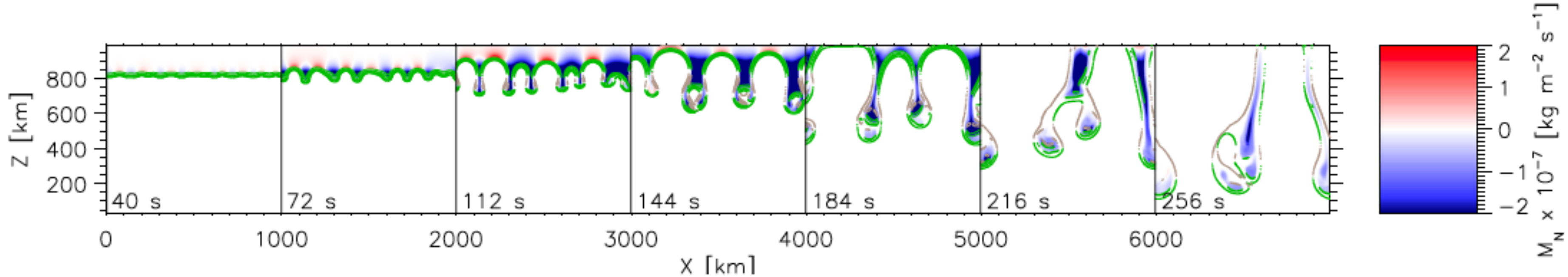

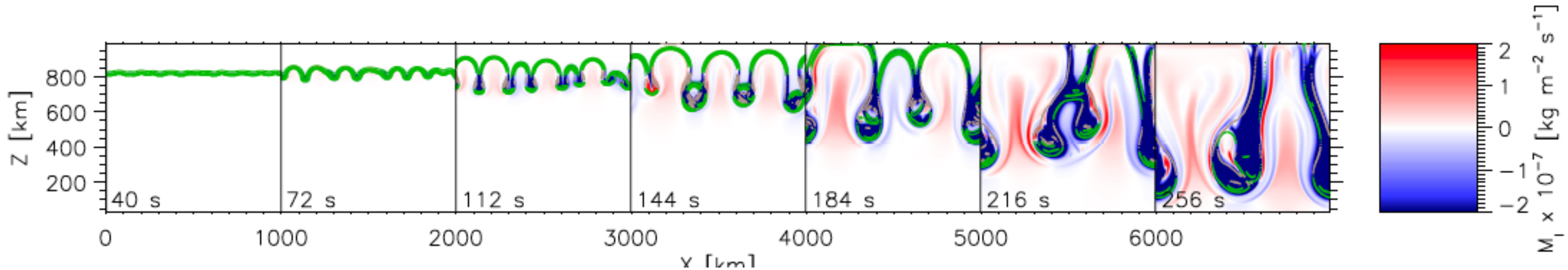

Summary

General dynamics

•Asymmetric velocity distribution; up flows are faster;

•Upflowing bubbles are more apparent in density images;

•Drops falling at constant speed ~3-5 km s^{-1}.

Ambipolar vs MHD differences:

•Small scales grow faster with ambipolar term “on”;

•Larger speeds of bubbles in with ambipolar term “on”;

•Measurable diffusion velocities of the orders of a few km s^{-1};

•Temperature of bubbles is up to 30% different.